THE JOURNAL OF BIOLOGICAL CHEMISTRY VOL. 287, NO. 2, pp. 1290–1305, January 6, 2012
Published in the U.S.A.

Molecular and Cellular Effects of Tamm-Horsfall Protein Mutations and Their Rescue by Chemical Chaperones*

Received for publication, July 14, 2011, and in revised form, November 16, 2011 Published, JBC Papers in Press, November 23, 2011, DOI 10.1074/jbc.M111.283036

Lijie Ma[‡], Yan Liu[‡], Tarek M. El-Achkar[§], and Xue-Ru Wu[‡¶‖1]

From the Departments of [‡]Urology and [¶]Pathology, New York University School of Medicine, New York, New York 10016, [‖]Veterans Affairs New York Harbor Healthcare System, Manhattan Campus, New York, New York 10010, and [§]Division of Nephrology, Saint Louis University and Saint Louis Veterans Affairs Medical Center, St. Louis, Missouri 63108

Background: Mutations of Tamm-Horsfall protein (THP) cause hereditary kidney diseases with unclear mechanisms.
Results: Cysteine-altering THP mutants bind, trap, and reduce the apical release of wild-type THP, effects that can be ameliorated by various chemical chaperones.
Conclusion: Intermolecular interactions between mutant and wild-type THP may affect disease phenotype.
Significance: Chemical chaperones may be of therapeutic value in THP mutation-caused diseases.

Correct folding of a nascent polypeptide in the lumen of the endoplasmic reticulum (ER) into a three-dimensional conformation is a crucial step in the stability, intracellular trafficking, and targeting to the final destination of a protein. By transiently and stably expressing human-relevant mutants of Tamm-Horsfall protein in polarized Madin-Darby canine kidney cells, we show here that a cysteine-altering mutation in the evolutionally conserved cysteine-rich domain had more severe defects in ER exit and surface translocation and triggered more apoptosis than a cysteine-altering mutation outside the domain. Both mutants were able to specifically bind and trap the wild-type Tamm-Horsfall protein (THP) and prevent it from exiting the ER and translocating to the cell surface. This explains at least partly why in patients with THP-associated diseases there is a marked urinary reduction of both the mutant and the wild-type THP. Exposure of mutant-expressing cells to low temperature (30 °C), osmolytes (glycerol, trimethylamine *N*-oxide, and dimethyl sulfoxide), and the Ca^{2+}-ATP inhibitor thapsigargin only slightly relieved ER retention and increased surface targeting of the mutants. In contrast, sodium 4-phenylbutyrate and probenecid, the latter a uricosuric drug used clinically to treat gout, markedly reduced ER retention of the mutants and increased their surface translocation and secretion into the culture media. The rescue of the THP mutants was associated with the restoration of the level and subcellular localization of cytosolic chaperone HSP70. Our results reveal intricate mechanistic details that may underlie THP-associated diseases and suggest that novel therapeutics enhancing the refolding of THP mutants may be of important value in therapy.

Tamm-Horsfall protein (THP[2]; also named uromodulin) is a kidney-specific protein made by the epithelial cells lining the thick ascending limb of the loop of Henle (1–4). Within these cells, THP is synthesized on the rough endoplasmic reticulum (ER). After proper folding, modification with high mannose glycomoieties, and addition of a C-terminal glycophosphatidylinositol, the protein exits the rough ER and transits to the Golgi apparatus where it is further modified with complex-type carbohydrates and then destined for the apical plasma membrane (5, 6). Mature THP is believed to anchor via its glycophosphatidylinositol tail onto the luminal leaflet of the lipid bilayer of the apical membrane of the thick ascending limb of the loop of Henle, although a recent study found the protein also to be associated with the primary cilia and the mitotic spindle poles of these tubular cells (7). Apically located THP is eventually released by proteases and/or phospholipases into the urine where it constitutes the most abundant urinary protein in most mammals (8–10). Evidence is mounting from genetically engineered models that urinary THP is indispensable for urinary tract defenses as its loss predisposes mice to urinary tract infections and mineral crystallization (11–18). The exact role(s) THP plays in renal physiology remains somewhat enigmatic. Recent genetic linkage studies show that certain polymorphisms of the THP gene have strong association with chronic kidney disease and nephrolithiasis in humans (19–22).

Among the key structural features of THP is its high cysteine content. Of the 590 amino acid residues in the mature protein (excluding the signal peptide and glycophosphatidylinositol consensus sequence), 48 are cysteines. Many of these cysteines are thought to be involved in forming disulfide bridges that stabilize the conformation of the protein. In particular, the cysteines inside the so-called "domain of 8 cysteines" (D8C) appear to be the most conserved among several structurally related proteins (23). It has been postulated that these 8 conserved cysteines can form four pairs of disulfide bonds and that failure to do so could lead to deleterious effects during the initial phase of THP synthesis. However, concrete experimental evidence is lacking. THP also has a tendency to polymerize via its zona pellucida domain and interdomain linker regions (24, 25).

* This work was supported, in whole or in part, by National Institutes of Health Grant DK56903.

[1] To whom correspondence should be addressed: Dept. of Urology, New York University School of Medicine, Veterans Affairs Medical Center in Manhattan, 423 E23 St., Rm. 18064 S., New York, NY 10010. Fax: 212-951-5424; E-mail: xue-ru.wu@med.nyu.edu.

[2] The abbreviations used are: THP, Tamm-Horsfall protein; MDCK, Madin-Darby canine kidney; ER, endoplasmic reticulum; D8C, domain of 8 cysteines; 4-PBA, sodium 4-phenylbutyrate; IP, immunoprecipitation; PLC, phospholipase C; FL, FLAG; TMAO, trimethylamine *N*-oxide.

However, at which stage of THP synthesis the intermolecular interactions take place and whether intermolecular disulfide bonds play a role in this process are unknown.

The importance of THP in renal diseases had not been fully appreciated until mutations of this protein were discovered in a group of hereditary diseases encompassing familial juvenile hyperuricemic nephropathy, medullary cystic kidney disease type II, and glomerulocystic kidney disease (4, 26–29). Transmitted in an autosomal dominant manner, these complex tubulointerstitial diseases share several clinical features including salt wasting, inability to concentrate urine, high serum uric acid and gout, and progressive renal failure. However, it is also recognized that despite a shared genetic cause, *i.e.* mutations in a single (THP) gene, tremendous heterogeneities exist among different disease entities, renal pathology, disease onset, and timeline of progression to renal failure (30–32). It has been suggested that THP mutation-associated renal diseases are a disease complex or a syndrome and that they are probably more appropriately labeled as "uromodulin storage diseases" (28).

A compilation of the THP mutations identified to date shows that over 90% are missense mutations, and over 60% affect the cysteines (6, 33). Given the general importance of disulfide bridges in stabilizing protein conformation, it has been hypothesized that THP mutations, in particular cysteine-altering mutations, can result in THP misfolding and delayed or failed ER exit (23). This has indeed turned out to be the case. When transfected into cultured epithelial cells, considerable amounts of mutation-bearing THPs become trapped in the ER. The mutants are not as efficient as their wild-type counterpart to reach the cell surface and be released into the media (6, 30, 34–36).

Notwithstanding the significant advances, several issues remain to be elucidated. For instance, are cysteines within the D8C conformationally more pivotal than those outside the domain? In other words, will replacing a cysteine in D8C with a non-cysteine residue lead to a more profound effect(s) than replacing one outside? With rare exceptions, THP mutations affect only one of the parental alleles, leaving the other allele (*i.e.* wild type) unaffected. Because both alleles of most genes are transcribed, this implies that the protein product of the mutant THP allele may exert a dominant-negative effect on the protein product of the wild-type THP allele. Patients with THP mutation-related diseases do have a profound reduction of not only the mutant but also the wild-type protein in the urine (35, 37, 38). Is this due to a reduced synthesis of the wild-type THP because of mutant-caused ER stress, or can it also be attributed to a trapping effect due to mutant/wild-type THP interaction? Additionally, because normal THP is located not only at the apical plasma membrane but also at the mitotic spindle poles (7), would a mutated THP compromise cell division and hence proliferation? Moreover, given the fact that THP mutation-caused diseases belong to the ER storage diseases, it will be important to explore whether there are potential therapeutics that can be used to improve the folding and cell surface targeting of THP mutants. A range of experimental conditions including permissive temperatures, osmolytes, small molecules, and chemical chaperones has been evaluated for several non-THP ER storage diseases (39, 40). Will THP mutants respond to some of these conditions, and if so, what is the underlying cellular mechanism(s)? The present study was designed to address some of these questions.

EXPERIMENTAL PROCEDURES

Construction of Expression Vectors

A full-length cDNA encoding mouse THP in pCMV-Sports 6 vector was obtained from American Type Cell Culture (ATCC, Manassas, VA). To help distinguish THP mutants from wild-type (WT) THP in co-transfection studies, we chose to introduce into THP cDNA well characterized small tags (*i.e.* hemagglutinin (HA; 9 amino acids) or FLAG (8 amino acids)) for which specific antibodies were commercially available. To avoid potential untoward effects and after pilot analyses, we selected a tag insertion site between residues 59 and 60 of the THP, a site significantly away from the signal peptide cleavage site, cysteine residues, and Asn-linked glycosylation sites. PCR was carried out using the THP cDNA as the template with a sense primer at the 5′-end of the coding region of the THP cDNA (5′-AGA GTG TAA AGG ATG GGG ATC-3′ (S-1)) and an antisense primer that spanned residues 59/60 and contained the HA sequence (5′-GTC CTC ACA CAC CAG CCC AGC GTA ATC TGG AAC ATC GTA TGG CTA ATC ACC AGT GAA GCC GGT C-3′ (AS-1) where the underline denotes the HA complementary sequence). A parallel round of PCR was carried with a sense primer complementary to AS-1 (5′-ACC GGC TTC ACT GGT GAT TAC CCA TAC GAT GTT CCA GAT TAC GCT GGG CTG GTG TGT GAG GAC-3′ (S-2)) and an antisense primer complementary to the 3′-end of the coding region of the THP cDNA (5′-CCA TCA TTG AAC CAT GAA GAT C-3′ (AS-2)). Products of the two rounds of PCR were mixed in equal proportions, denatured, reannealed, and extended to full length using a DNA polymerase reaction mixture. A third round of PCR was performed using primers S-1 and AS-2 to generate a full-length THP cDNA containing the HA tag, and the PCR product was subcloned into pGEM-T vector (Promega, Madison, WI) and then cloned into mammalian expression vector pcDNA3.0 between the SacII and NotI sites. The introduction of FLAG tag into THP cDNA followed identical procedures at the same site (between residues 59 and 60) with the exception that FLAG-specific primers were used at the insertion site.

Site-directed mutagenesis to mutate codons 126 and 217 of THP was carried out using as template pcDNA3.0 vector bearing the THP-HA or the THP-FLAG using a QuikChange kit from Stratagene (La Jolla, CA). The primer pairs used were as follows: (i) for codon 126: sense, 5′-GCC CTG GCC ACC CGT GTC AAC ACA G-3′; antisense, 5′-CTG TGT TGA CAC GGG TGG CCA GGG C-3′ where the underline denotes the converted cysteine to arginine (C126R); and (ii) for codon 217: sense, 5′-ATG GCT GAG ACC GGT GTG CCC GTC C-3′; antisense, 5′-GGA CGG GCA CAC CGG TCT CAG CCA T-3′ where the underline indicates converted cysteine to glycine (C217G). The modified cDNAs were completely sequenced to establish the presence of the HA and FLAG tags, the presence of specific mutations (*i.e.* C126R and C217G), and the absence of PCR-introduced artifact. A total of seven expression vectors

were created: WT-no tag, WT-HA, WT-FLAG, C126R-HA, C126R-FLAG, C217G-HA, and C217G-FLAG (see Fig. 1).

Transient and Stable Transfection

The Madin-Darby canine kidney (MDCK) cell line (ATCC) was expanded in low glucose Dulbecco's minimal essential medium (DMEM; Invitrogen) supplemented with 10% fetal bovine serum and 100 μg/ml streptomycin at 37 °C with 5% CO_2. RT-PCR, Western blotting, and immunofluorescence staining did not detect any endogenous THP expression in this cell line. For transient transfection, 5×10^4 cells were plated into 24-well cell culture plates, and 16 h later, the attached cells were transfected separately with the aforementioned seven expression vectors using Lipofectamine 2000 (Invitrogen) at a 2 μg of DNA/2 μl of reagent ratio per 1×10^5 cells. For transient co-transfection, a 1:1 ratio (1 μg/1 μg) of the co-transfected plasmids was used.

For obtaining stably transfected clones, overnight cultures of MDCK cells were transfected with the aforementioned plasmids following the same procedure. Forty-eight hours later, the culture medium was switched to DMEM containing G418 at a final concentration of 1 mg/ml. The cells were maintained in this condition with a change of fresh medium every 2 days for a week. The surviving cells were digested with 0.25% EDTA, trypsin and diluted to ~100 cells/10-cm culture dish for continued culture in the G418 selective medium for 4 more weeks. Single cells were then selected for subculture and expansion into stable cell lines.

Fluorescence-activated Cell Sorting

Live MDCK Cells Transfected with WT and Mutated THPs—Stably transfected cells that had been subcultured for 48 h were collected in DMEM with 10% fetal bovine serum to 1×10^6 cells/ml. The cells were incubated at 4 °C for 30 min with a chicken anti-HA antibody (1:1,000 dilution; Millipore, Billerica, MA). After washing, the cells were incubated at 4 °C for 30 min with goat anti-chicken FITC (1:500 dilution; Abcam). After further washing, the cells were incubated at room temperature for 10 min with 7-aminoactinomycin D to exclude nonviable cells. Cell sorting was carried out by flow cytometry (FACSCalibur) and analyzed with CellQUEST software (both from BD Biosciences).

Cell Cycle Distribution—Stably transfected MDCK cells expressing WT THP, WT-HA, C126R-HA, or C217G-HA (1×10^5 cells for each line) were cultured for 48 h. Harvested cells were fixed in 100% ice-cold ethanol and after washing were treated with RNase (30 mg/ml) and then with 1 mg/ml propidium iodine followed by fluorescence-activated cell sorting (FACS) analysis.

Apoptotic Cells—Annexin V-PE Apoptosis Detection Kit I (BD Bioscience) was used to quantify apoptotic cells. Briefly, stably transfected MDCK cells expressing the WT-HA, C126R-HA, or C217G-HA were cultured for 48 h. The cells were washed twice in ice-cold PBS, washed once in 1× "binding buffer," and then supplemented with 5 μl of annexin V-phycoerythrin and 5 μl of 7-aminoactinomycin D (in 100 μl of cell suspension (1×10^5 cells)). The FACS was performed according to the manufacturer's instructions.

Immunofluorescence Labeling and Western Blotting

Transiently or stably transfected cells were fixed either in 4% PBS-buffered paraformaldehyde at room temperature (RT) for 15 min to produce non-permeabilized cells or in an ice-cold methanol/acetone mixture (1:1 ratio) on ice for 15 min to produce permeabilized cells. After blocking of nonspecific sites with 3% bovine serum albumin in PBS at RT for 30 min, the cells were incubated with chicken anti-HA (1:500 dilution) followed by goat anti-chicken FITC to detect HA-tagged THP. Alternatively, the cells were incubated with rabbit anti-FLAG (1:500 dilution) followed by goat anti-rabbit rhodamine. For double staining, the two staining systems were combined. For the assessment of whether THP mutant expression in MDCK cells would have a general negative effect on the cell surface targeting of endogenous membrane proteins, mouse monoclonal antibody against GP135, a well established cell surface marker of MDCK cells, was used as an internal control during double immunofluorescence staining (courtesy of Dr. George Ojakian of SUNY Downstate Medical Center, Brooklyn, NY; Ref. 41). For caspase 3 staining, permeabilized, stable cell lines expressing WT-HA, C126R-HA, and C217G-HA were exposed to rabbit anti-caspase 3 antibody (1:200 dilution; Cell Signaling Technology, Danvers, MA) and then to goat anti-rabbit rhodamine. For detection of heat shock protein 70 (HSP70), 1×10^4 stably transfected MDCK cells expressing WT-HA, C126R-HA, or C217G-HA were treated with low temperature, sodium 4-phenylbutyrate (4-PBA), and probenecid for 48 h. The cells were permeabilized and double stained with primary antibodies mouse anti-HSP70 (1:200 dilution; Millipore) and rabbit anti-THP (1:500; Ref. 42) followed by secondary antibodies goat anti-mouse FITC and goat anti-rabbit rhodamine.

For Western blotting, protein samples were dissolved in SDS loading buffer containing 10% β-mercaptoethanol and resolved by SDS-PAGE (10% acrylamide gel for THP and chaperones, 12% gel for caspase 3, and 4–12% gradient gel for the co-immunoprecipitation (IP) experiment (see below)). After electrophoresis, the proteins were electrotransferred onto the Immobilon PVDF membrane, incubated consecutively with primary and horseradish peroxidase-conjugated secondary antibodies, and visualized by an enhanced chemiluminescence method. All antibodies against the ER chaperones were obtained from Cell Signaling Technology and used after dilutions (rabbit anti-ERp57, 1:500; rabbit anti-calnexin, 1:500; rabbit anti-calreticulin, 1:500).

Co-immunoprecipitation

Stably transfected MDCK cells harboring a mutated THP (either C216R-HA or C217G-HA) were secondarily transfected with a plasmid containing the wild-type THP cDNA (WT-FLAG). After 48 h, the cells were lysed with radioimmune precipitation assay buffer (1% (octylphenoxy)polyethoxyethanol, 50 mM Tris/HCl, pH 7.4, 150 mM NaCl, 0.5% deoxycholate, 0.1% SDS, 2 mM EDTA, and 0.5 mM PMSF). The lysate was centrifuged, and the supernatant was incubated with a rabbit anti-FLAG antibody (2 μg of antibody/100 μg of total protein) at 4 °C for 1 h. The mixture was then supplemented with 20 μl of Protein G PLUS-agarose and incubated on a rocker platform at

4 °C overnight. The agarose beads were collected by centrifugation at 1,000 × *g* at 4 °C for 5 min and washed four times with PBS. After the final wash, the beads were resuspended in 1× electrophoresis loading buffer, boiled for 3 min, and subjected to SDS-PAGE. Western blotting was carried out using chicken anti-HA antibody followed by goat anti-chicken HRP. In a reverse co-immunoprecipitation experiment, the same protein lysate was incubated with a chicken anti-HA antibody followed by identical precipitation procedures; Western blotting was done using a rabbit anti-FLAG antibody and goat anti-rabbit HRP.

Enzyme-linked Immunoabsorbent Assay

ELISA was used to quantify THP released into the culture media. Briefly, microtiter wells were coated with 200 μl of media from cells cultured for 6, 20, 30, 40, and 60 h, and unbound proteins were removed by washing the wells with PBS. The following solutions were then added consecutively with intervening washing steps: (i) blocking solution (3% milk made in PBS), (ii) sheep anti-THP antibody (1:3,000 dilution), and (iii) rabbit anti-sheep HRP (1:6,000 dilution). After the final wash, substrate for HRP was added and developed for 20 min after which the reaction was stopped by the addition of 2 M H_2SO_4. The plates were read at 450 nm, and readings were plotted against a standard curve generated using purified THP from pooled healthy human urine.

Phospholipase C Treatment

For assessing whether mutant THPs interact with and reduce the cell surface targeting of WT THP, stably transfected MDCK cells (1×10^5/well) expressing the FLAG-tagged WT THP were transfected with HA-tagged THP mutants (2 μg each of C126R-HA or C217G-HA). As a control, the same stably transfected MDCK cells expressing the FLAG-tagged WT THP were transfected with HA-tagged WT THP (WT-HA). Forty-eight hours later, the cells were washed and incubated with phospholipase C (Sigma) in PBS (3 units/100 μl of cell suspension) at 37 °C for 4 h. The supernatant was collected by centrifugation at 1,000 × *g* for 5 min, and the same volume of each supernatant (10 μl/well) was subjected to ELISA using rabbit anti-FLAG as the primary antibody. Because HA standard was not available, OD readings at 450 nm were used to represent the relative abundance of phospholipase C (PLC)-cleavable WT-FLAG.

Proteosome Inhibition

MDCK cells stably transfected with C126R-HA or C217G-HA were cultured for 24 h and then changed to fresh DMEM or DMEM plus proteasome inhibitor MG132 (Sigma) (43) to a final concentration of 10 μM. Cell culture continued for another 12 h before the cells were fixed in 4% paraformaldehyde at 4 °C for 10 min followed by permeabilization in 0.05% Triton X-100 at 4 °C for 10 min. Double immunofluorescence staining was then carried out using anti-HA and anti-HSP70 followed by secondary antibodies conjugated with Alexa Fluor 488 and Alexa Fluor 594.

Rescue of THP Mutants by Low Temperature, Osmolytes, and Chemical Chaperones

Stably transfected MDCK cells were cultured for 16 h in low glucose DMEM containing 10% fetal bovine serum, 100 IU/ml penicillin, 100 μg/ml streptomycin, and 1 mg/ml G418. The cells were washed three times with serum-free low glucose DMEM and treated with fresh DMEM containing 10% fetal bovine serum and each of the following conditions/agents: 1) low temperature (30 °C); 2) 1% glycerol; 3) 5 mg/ml trimethylamine *N*-oxide (Sigma-Aldrich); 4) 1% DMSO; 5) 1 μM thapsigargin (Sigma); 6) 10 mM sodium 4-phenylbutyrate (Biovision); and 7) 1 mg/ml probenecid. The cells were cultured for another 48 h and then subjected to immunofluorescence staining and FACS using chicken anti-HA antibody. In parallel experiments, the culture media were subjected to ELISA using sheep anti-THP as the primary antibody and purified human THP as a standard. Finally, treated cells were analyzed for the expression of selected protein chaperones by Western blotting and immunofluorescence staining using antibodies against ERp57 (1:500 dilution; Cell Signaling Technology), calnexin (1:500; Cell Signaling Technology), calreticulin (1:500; Cell Signaling Technology), and HSP70 (1:500; Millipore).

RESULTS

Cysteine-altering Mutation in D8C of THP Causes More Severe ER Retention and Less Cell Surface Translocation than Another Outside of Domain—To better understand the molecular and cellular effects of THP mutations and to set the stage for testing novel therapeutics for THP mutation-associated diseases, we constructed a series of mammalian expression vectors bearing (i) a WT THP cDNA, (ii) a THP cDNA harboring a missense mutation at codon 126 that converted cysteine to arginine (*i.e.* C126R), and (iii) a THP cDNA harboring a missense mutation at codon 217 that converted cysteine to glycine (*i.e.* C217G). Notably, Cys-126 resides in the third EGF-like domain of THP, whereas Cys-217 resides within the evolutionarily conserved D8C (23). These two mutants were selected also because they are frequently present in human THP mutation-caused diseases (28, 44). To facilitate the distinction between the mutant THP and the WT THP, we engineered small tags (HA or FLAG) that have been well characterized *in vitro* and *in vivo* into the WT and mutant THP. After pilot analyses, we selected the site between residues 59 and 60 as the tag insertion site, which was away from the signal peptide cleavage site, cysteine residues, and Asn-linked glycosylation sites. Transient transfection of these vectors into polarized MDCK cells showed that the HA- or FLAG-tagged THP translocated to the cell surface as efficiently as the tagless THP as evidenced by the immunofluorescence staining of non-permeabilized cells (Fig. 1*A*) and live cell sorting (Fig. 1*B*; also see later text). This indicated that the presence of the tags did not affect THP biosynthesis, intracellular trafficking, and cell surface targeting. In stark contrast, the two THP mutants (C126R and C217G) had considerably lower cell surface staining in non-permeabilized cells, and their intracellular staining in permeabilized cells was predominantly perinuclear (Fig. 1*A*). Large irregular aggregates were also apparent. These results are consistent with several pub-

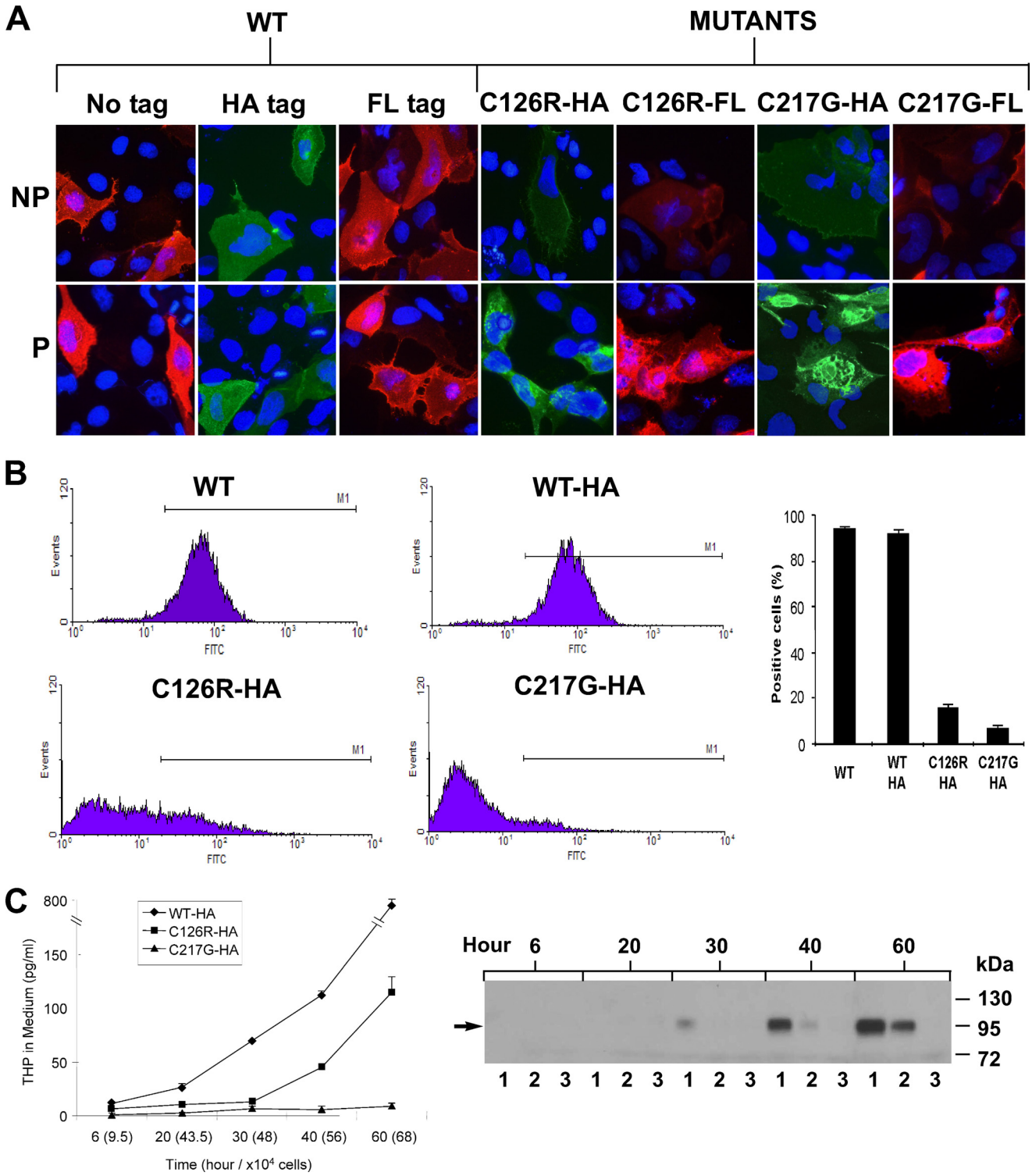

FIGURE 1. **Localization of WT and mutated THP in transiently and stably transfected MDCK cells.** *A*, cultured MDCK cells were transiently transfected with WT THP or THP bearing point mutations at two independent sites (*i.e.* C126R and C217G). Transfected cells were subjected to immunofluorescence staining under non-permeabilized or permeabilized conditions. *B*, *left four panels*, stably transfected cell lines harboring untagged wild-type THP or HA-tagged WT THP, C126R THP mutant, or C217G THP mutant were subjected to fluorescence-activated cell sorting using anti-THP antibody (for untagged wild-type THP) or anti-HA antibody (for all HA-tagged proteins) in conjunction with a FITC-labeled secondary antibody. *M1* denotes the window of sorted live cells. *Right panel*, a bar diagram summary of the *left four panels* (means ± S.E.). *C*, detection of THP secreted in culture media by ELISA (*left panel*) (means ± S.E.) and Western blotting (*right panel*) using an anti-HA antibody. Culture media from stably transfected cell lines harboring HA-tagged WT and mutated THP (C126R or C217G) were collected at 6, 20, 30, 40, and 60 h postsubculture and were normalized based on the same cell numbers at each time point as indicated.

lished reports in which THP mutants at different sites were transiently expressed in MDCK and non-MDCK cells (6, 30, 34–36). Although both the THP mutants we tested became trapped in the ER, the severity was different: the C217G mutant had more profound perinuclear staining and weaker cell surface staining than the C126R mutant (Fig. 1*A*). FACS analysis of

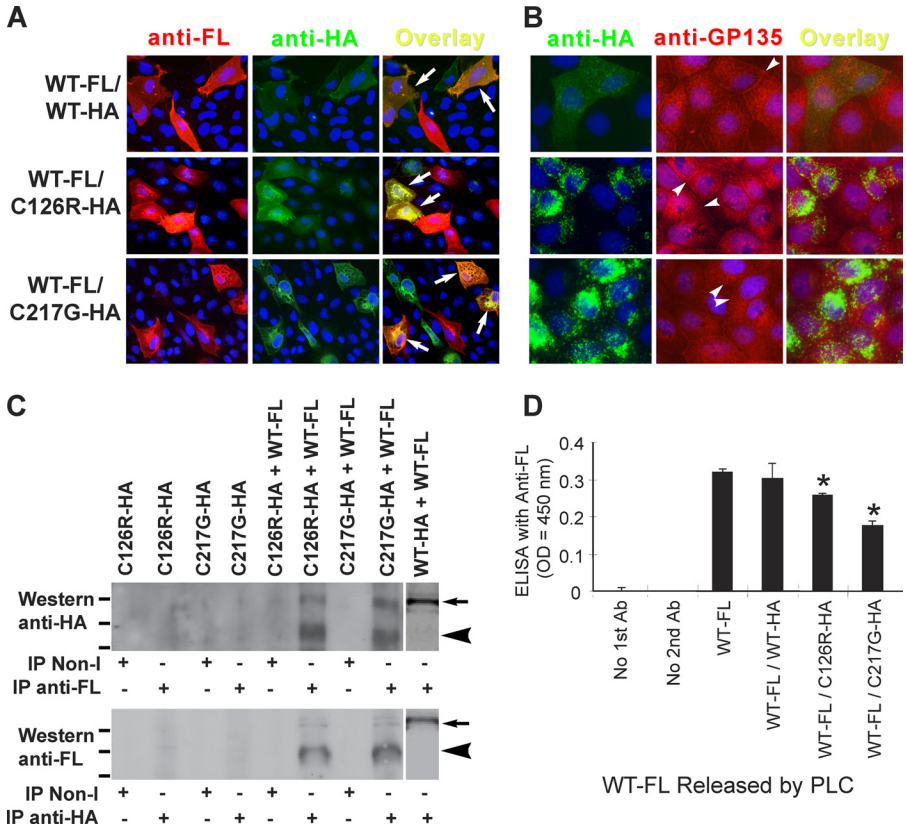

FIGURE 2. **Interaction of mutated THP with WT THP and resultant ER retention and reduced surface translocation of WT THP.** *A*, co-expression of WT and mutant THP by double transfection. Cultured MDCK cells were transiently transfected simultaneously with an FL-tagged WT THP and an HA-tagged mutant THP (*i.e.* C126R or C217G (*middle* and *bottom panels*, respectively)). As a control, the cells were doubly transfected with an FL-tagged WT THP and an HA-tagged WT THP (*top panels*). The transfected cells were then permeabilized and double immunofluorescence-stained using primary antibodies against FL and HA followed by corresponding fluorescein-conjugated secondary antibodies (see "Experimental Procedures" for details). *Arrows* denote cell surface co-localization of WT-FL and WT-HA (*top right*); peri-nuclear co-localization of WT-FL and C126R-HA (*middle right*); and peri-nuclear co-localization of WT-FL and C217G-HA (*bottom right*). *B*, effect of THP mutant expression on the cell surface targeting of endogenously expressed GP135. MDCK cells doubly transfected with WT-FL/WT-HA (*top panels*), WT-FL/C126R-HA (*middle panels*), or WT-FL/C217G-HA (*bottom panels*) were permeabilized and double immunofluorescence-stained using primary antibodies against HA and GP135. *Arrowheads* denote surface membrane staining. *C*, demonstration of mutant and WT THP interaction by co-immunoprecipitation. Stably transfected cell lines harboring either HA-tagged C126R or HA-tagged C217G THP mutant were secondarily transfected with FL-tagged WT THP. IP was done using an anti-FL antibody followed by protein A-conjugated agarose beads. The precipitated products were detected by Western blotting using anti-HA antibody. Singly transfected, mutant-THP bearing cells were used as negative controls (the *first four lanes*), whereas cells doubly transfected with HA-tagged WT THP and FL-tagged WT THP were used as a positive control (the *last lane*). Reverse co-IP experiments were done using anti-HA antibody (to pull down THP mutants) followed by Western blotting using anti-FL antibody. In both types of co-IP experiments, isotype, non-immune IgGs (*Non-I*) were used as negative controls. *Short lines* at the *left edges* of both panels mark the positions of the molecular mass standard: from *top* to *bottom*, 95, 72, and 55 kDa. *Arrows* and *arrowheads* mark the fully and under-glycosylated species, respectively, of THP. *D*, influence of mutated THP on membrane surface translocation of WT THP as assessed by PLC treatment. MDCK cells stably transfected with FL-tagged WT THP were secondarily transfected with HA-tagged THP mutants. Singly (as controls) and doubly transfected cells were then treated with PLC, and the supernatant was subjected to ELISA using primary anti-FL antibody (*Ab*). Experiments were done in triplicate and data shown were means ± S.E. *Asterisks* denote differences with statistical significance *versus* WT-FL ($p < 0.05$).

stably transfected cells confirmed such a mutant-dependent difference in that only 7% of the cells harboring C217G expressed the protein on the cell surface compared with 16% of the cells harboring C126R (Fig. 1*B*). In further support of this, the amounts of THP released into the culture media at different time points of the stable cultures were markedly different between the two mutants (Fig. 1*C*). Both ELISA and Western blotting showed that over a 60-h culture period there was a steady increase in the concentrations of the WT-HA, a slower increase of C126R-HA reaching a detectable level by 40 h, and no increase at all of C217G over the entire period (Fig. 1*C*). These results, combined with those reported earlier (6, 30, 33–36), strongly suggest that THP mutations at different locations may exert different effects on protein folding, ER exit, and cell surface translocation and that mutations inside the evolutionally conserved D8C, particularly those altering the cysteines, may alter the conformational structure of THP more profoundly than those outside the domain.

Mutant THP Binds to and Traps Wild-type THP—To determine whether the mutated THP was capable of binding WT THP, thus exerting a dominant-negative effect, we carried out transient co-transfection of MDCK cells with (i) the plasmid encoding FLAG-tagged WT THP (WT-FL) along with the plasmid encoding HA-tagged C126R THP mutant (C126R-HA) and (ii) the plasmid encoding WT-FL along with the plasmid encoding HA-tagged C217G THP mutant (C217G-HA). Co-transfection of WT-FL and WT-HA was done in parallel as a control. Although, as expected, cells expressing both WT-FL and WT-HA exhibited exclusively cell surface staining (Fig. 2*A*, *top panel*), those cells expressing both WT-FL and C126R-HA exhibited perinuclear staining of not only C126R-HA but also WT-FL (Fig. 2*A*, *middle panel*, *arrows*, *yellow* color). The same

phenomenon was observed when C217G-HA was co-expressed with WT-FL (Fig. 2*A*, *bottom panel*, *arrows*). Such a trapping effect appeared to be mainly the result of mutant THP/WT THP interaction as the cell surface translocation of GP135, a well established cell surface membrane protein endogenously expressed by MDCK cells (41), was largely unaffected in mutant-expressing cells (Fig. 2*B*). These data demonstrated for the first time that the mutant THP interacts with the wild-type counterpart in the lumen of ER, being responsible at least partially for the ER retention of the WT THP (see later text).

To extend the immunofluorescence staining data, we performed co-immunoprecipitation on stably transfected MDCK cells harboring C126R or C217G that were secondarily transiently transfected with WT-FL. An anti-FL antibody was used for immunoprecipitation, and the precipitated products were subjected to Western blotting using an anti-HA antibody to determine whether the WT-FL was able to pull down mutant THPs. We found that the anti-FL antibody pulled down (via WT-FL/C126R-HA interaction) a minor (100-kDa) and a major (~65-kDa) protein species that reacted with the anti-HA antibody (Fig. 2*C*). The 100-kDa protein species corresponded to the fully glycosylated, cell surface version of the THP as evidenced by co-transfection experiments with HA-tagged WT THP and FL-tagged WT THP (*last lane*) that did not affect the translocation of either protein. The 65-kDa protein species, on the other hand, corresponded most likely to the ER version that lacked the complex-type glycosylation. The co-IP experiments with the anti-FL antibody were highly specific because no protein was pulled down with singly transfected MDCK cells expressing only the C126R-HA or C217G-HA and because no protein was pulled down with an isogenic non-immune antibody. To take a step further, we used the same set of co-transfected cells to carry out a reverse co-IP experiment using the anti-HA antibody for co-IP and the anti-FL antibody for Western blotting to determine whether the mutant THPs were able to pull down the WT-FL. This indeed turned out to be the case (Fig. 2*C*, *lower panel*). More importantly, the fully glycosylated WT-FL (*i.e.* the cell surface version) also accounted for only a minor species of the precipitated WT-FL (*arrow*), again indicating that the majority of the WT-FL was trapped in the ER due to its interaction with the mutant THPs. Finally, we assessed whether the trapping effects of the THP mutants on the WT THP would lead to a reduction of WT THP released into the solution by PLC, an enzyme that cleaves the glycophosphatidylinositol linkage of THP (10). In this study, MDCK cells stably transfected with WT-FL were secondarily transiently transfected with C126R-HA or C217G-HA. Singly (controls) and doubly transfected cells were then treated with PLC, and the supernatant was subjected to ELISA using primary anti-FL antibody. A significantly reduced level of WT-FL was noted in cells co-expressing the WT and mutated THPs as compared with cells expressing the WT THP only or cells expressing differently tagged WT THP (Fig. 2*D*; *asterisks*, $p < 0.05$). An even more profound reduction of PLC-cleavable WT-FL was not observed mainly because of the relatively low secondary transfection efficiency with the mutant THPs compared with the high level of stably expressing of WT THP. Collectively, results from these independent but complementary experiments established that mutant THP interacts with the WT THP and prevents the latter from exiting the ER and translocating to the cell surface.

Mutant THP Accelerates Apoptosis but Does Not Alter Cell Proliferation—To assess whether the two THP mutants, which were trapped in the ER, affected cell proliferation and apoptosis and, if so, whether they did so to varied extents, we subjected stably transfected MDCK cells to FACS after propidium iodide and annexin V labeling. The steady-state distribution of all phases of the cell cycle (G_0/G_1, S, and G_2/M) of the cells expressing C126R-HA or C217G-HA were indistinguishable from the cells expressing WT or WT-HA, suggesting that the THP mutants did not reduce cell proliferation (Fig. 3, *A* and *C*). In contrast, significantly more cells expressing the mutants underwent apoptosis than the cells expressing the WT THP (Fig. 3*B*, compare *lower right quadrants*; also see Fig. 3*D*). Of the two THP mutants, C217G once again elicited more apoptotic responses (~10% of the cells) than C126R (~6% of the cells). Western blotting (Fig. 3*E*) and immunofluorescence staining (Fig. 3*F*) of caspase 3 independently confirmed the cell sorting results.

Low Permissive Temperature and Osmolytes Enhance Cell Surface Translocation of Mutated THP—Because the mutated THPs cause ER retention and apoptosis, it is likely that conditions ameliorating protein misfolding and enhancing ER exit will have a beneficial effect on cells bearing such mutations. Although low permissive temperature and osmolytes had been tested previously (39), few have been tested for THP mutants. We therefore cultured MDCK cells stably transfected with C126R-HA or C217G-HA in low permissive temperatures (<37 °C) and in various concentrations of osmolytes including glycerol, trimethylamine *N*-oxide (TMAO), and DMSO. Fig. 4 shows the immunofluorescence labeling and live cell sorting (FACS) via the cell surface THP under the culture conditions that resulted in the maximal surface labeling (*i.e.* 30 °C, 1% glycerol, 5 mg/ml TMAO, and 1% DMSO). Compared with non-treated cells, which had little if any cell surface labeling under non-permeabilized condition, cells cultured under the four conditions became more intensely surface-labeled (Fig. 4). Punctate surface labeling was seen with both glycerol and TMAO treatments, whereas uniform surface labeling was associated with low temperature and DMSO treatments. Consistent with the increased surface labeling, there was generally a reduction of perinuclear staining in all the conditions as evidenced by staining with permeabilized cells. Overall, TMAO and DMSO treatments performed slightly worse than low temperature and glycerol. Despite their different degrees of ER retention and surface translocation, the C126R-HA and C217G-HA mutants seemed to have responded similarly to the four conditions (Figs. 4 and 6, *A* and *C*). The increase in surface translocation also translated into an increased release of mutated THPs into the culture medium as evidenced by ELISA analysis (Fig. 6*C*). However, such increases (*e.g.* ~25% of the WT THP) did not parallel the increase in surface labeling (>50%) by FACS (Fig. 6*A*). This might have been due to the fact that cells expressing even a small amount of mutated THP on the surface can be sorted, but in this case, only a small amount of protein could be released into the medium. Another possibility is that THP mutants that have translocated to the cell surface are less efficiently cleaved than the WT THP, although the second possibility is less likely based on our immunofluorescence staining data.

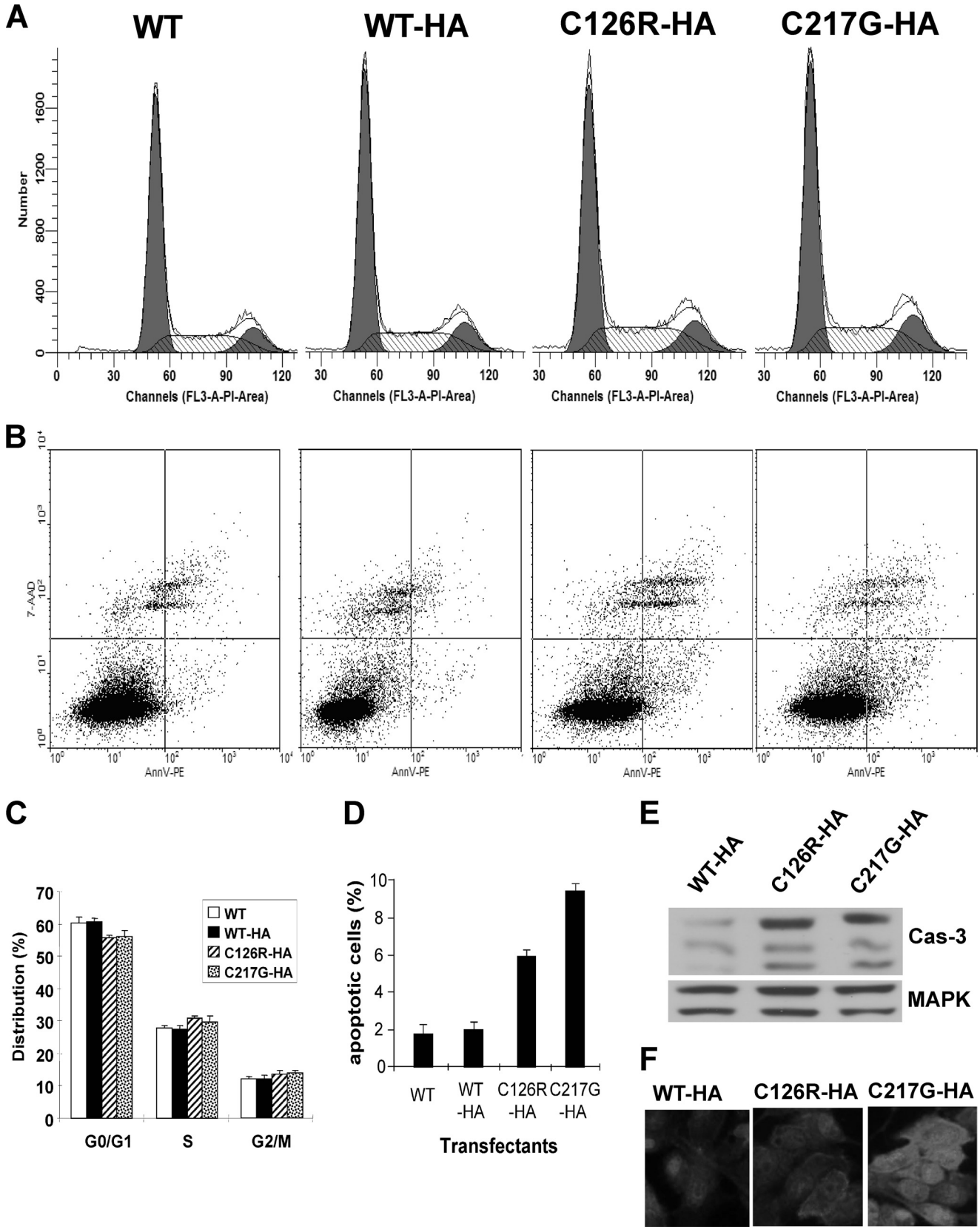

FIGURE 3. **Cell cycle and apoptotic status of MDCK cells harboring THP mutants.** MDCK cells stably transfected with WT THP, WT THP tagged with HA, or mutated THP (C126R or C217G) tagged with HA were stained with propidium iodide (*PI*) and subjected to FACS (*A*) or incubated with annexin V (*AnnV*) followed by FACS (*B*). The *filled curves* in *A* represent the G_0/G_1 (the *first peak*) and G_2/M (the *second peak*) phases. The *hatched curve* represents the S phase. *Bottom right quadrants* in *B* represent apoptotic cells. *C* and *D*, summary of cell cycle and apoptotic status. Data were means ± S.E. *E* and *F*, Western blotting and immunofluorescence detection of caspase 3 (*Cas-3*) showing higher levels of precursor (*top band* in *E*) and activated caspase 3 (*middle* and *lower bands* in *E*) in MDCK cells expressing the THP mutants than in those expressing the WT THP. *7-AAD*, 7-aminoactinomycin D; *PE*, phycoerythrin.

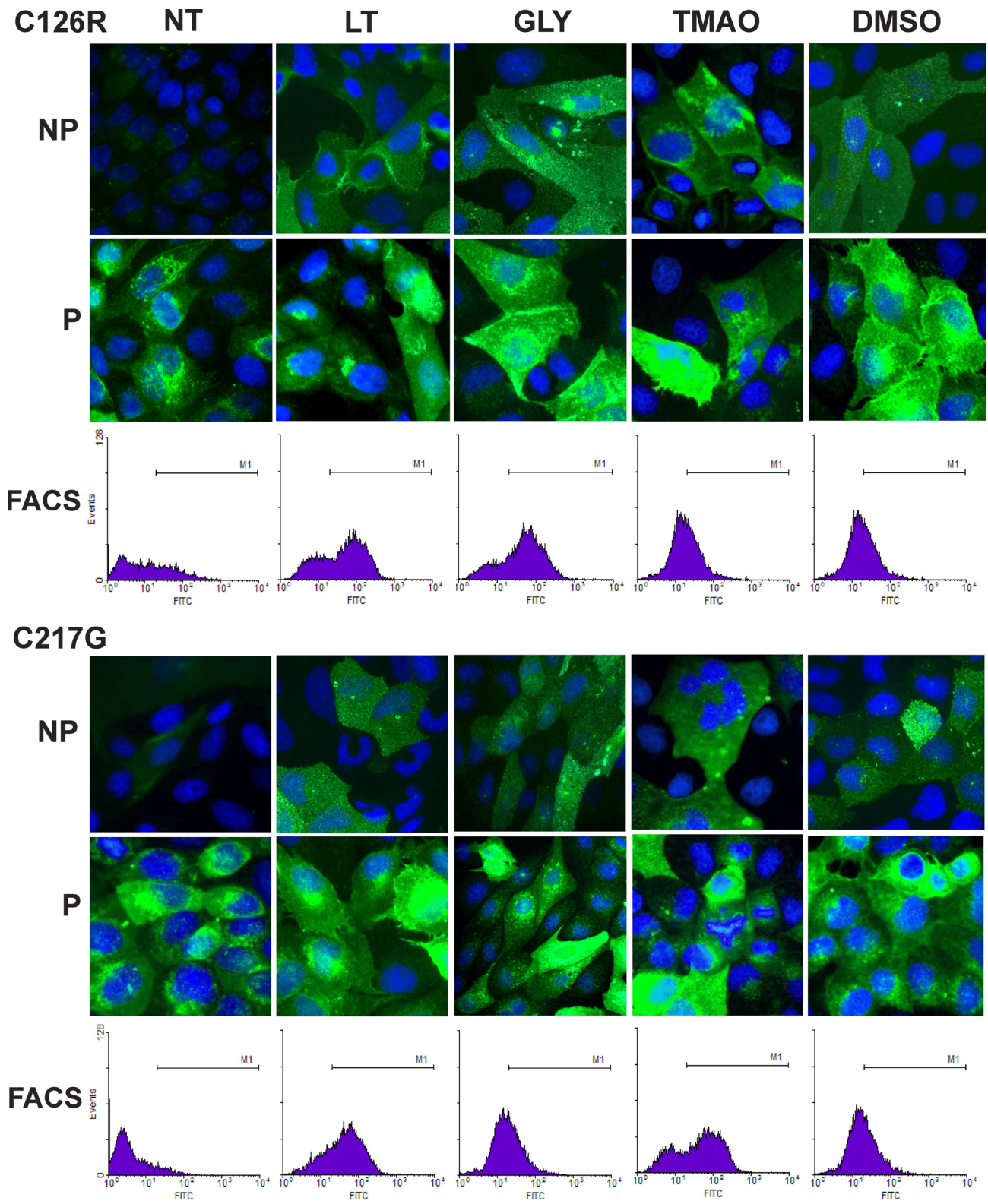

FIGURE 4. **Effects of permissive temperature and osmolytes on ER exit and cell surface translocation of THP mutants.** MDCK cells stably transfected with the two HA-tagged THP mutants (C126R (*top three panels*) or C217G (*bottom three panels*) underwent no treatment (*NT*) or were treated with low temperature (*LT*; 30 °C), glycerol (*GLY*), TMAO, and DMSO. Forty-eight hours after treatment, non-permeabilized (*NP*) and permeabilized (*P*) cells were immunofluorescence-stained with an anti-HA antibody. Alternatively, live cells underwent FACS using the anti-HA antibody, and nuclei were counterstained with DAPI. *M1* in the *FACS panels* represents sortable live cells (expressing surface THP).

Chemical Chaperones Significantly Improve ER Exit and Cell Surface Targeting of Mutated THP—Although low permissive temperature and osmolytes showed positive effects on reducing perinuclear accumulation of THP mutants and improving surface translocation, these reagents/conditions are either toxic or not suitable for *in vivo* applications (39). Additionally, their

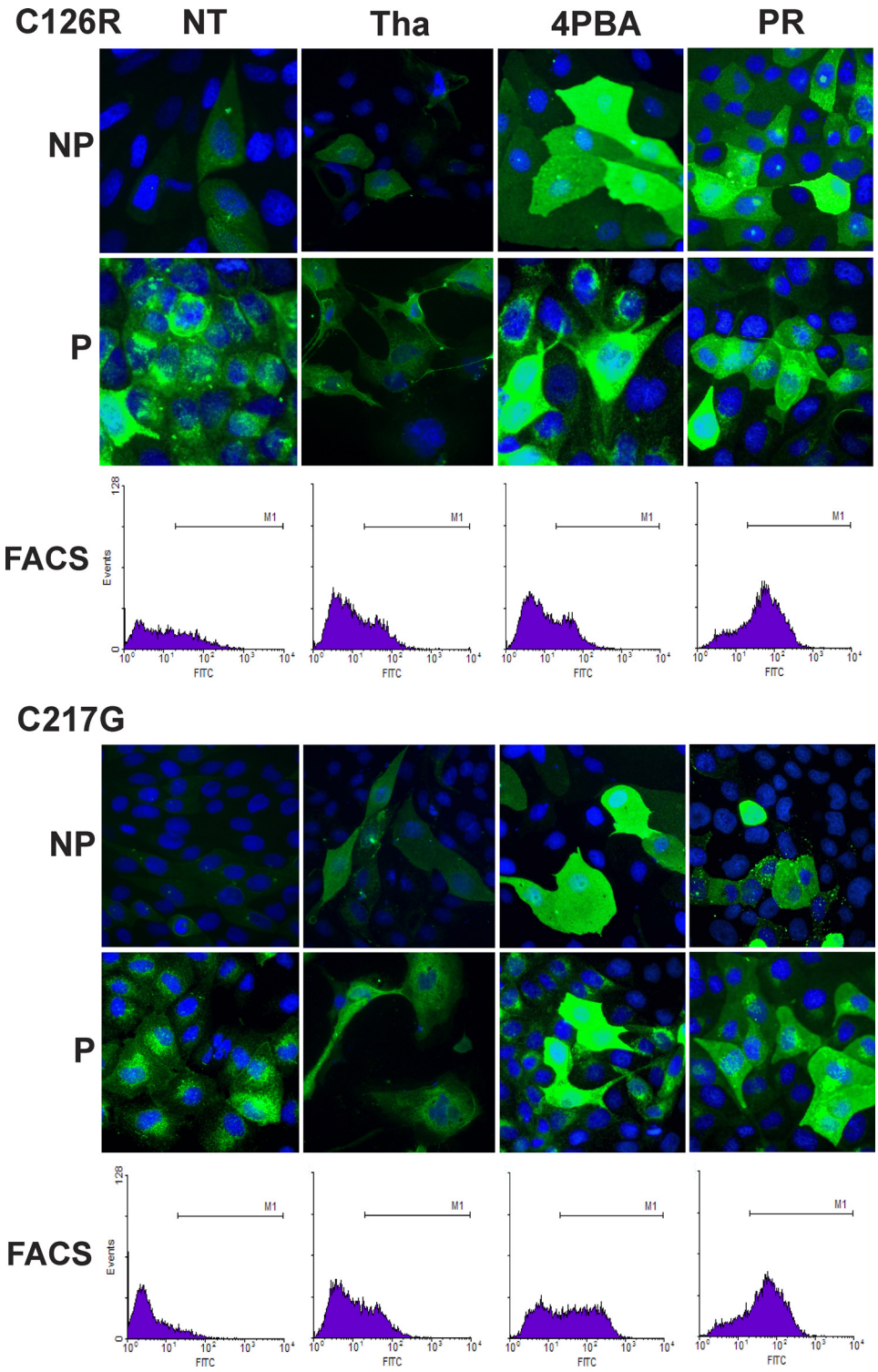

FIGURE 5. **Effects of small molecule chemical chaperones on ER exit and cell surface translocation of THP mutants.** MDCK cells stably transfected with the two HA-tagged THP mutants (C126R (*top three panels*) or C217G (*bottom three panels*) underwent no treatment (*NT*) or were treated with thapsigargin (*Tha*), 4-PBA, or probenecid (*PR*). Forty-eight hours after treatment, non-permeabilized (*NP*) and permeabilized (*P*) cells were immunofluorescence-stained with an anti-HA antibody. Alternatively, live cells underwent FACS using the anti-HA antibody. *M1* in the *FACS panels* represented sortable cells (expressing surface THP).

effects only seemed marginal (Figs. 4–6). We therefore evaluated several chemical chaperones/small molecules for their effects on the THP mutants using the same experimental system. These included thapsigargin, a small molecule that inhibits its Ca^{2+}-ATPase and the Ca^{2+}-dependent quality control mechanism by the molecular chaperones (45); 4-PBA, a chemical chaperone that increases the expression of heat shock proteins (46); and probenecid, a drug used clinically to treat hyperuricemia (47). Fig. 5 shows the results from the best conditions for each agent (*i.e.* 1 μM thapsigargin, 10 mM 4-PBA, and 1

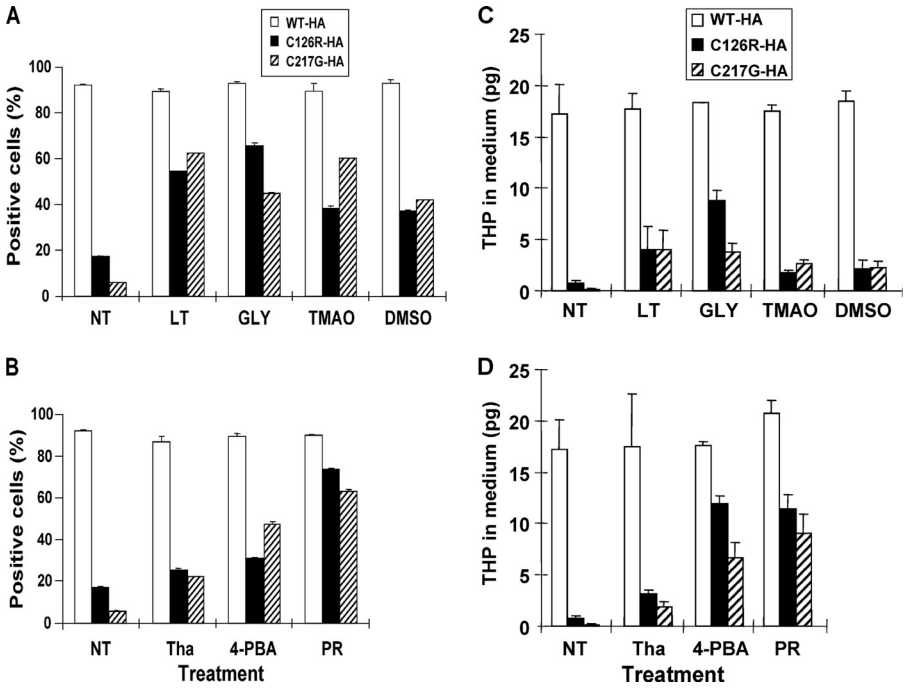

FIGURE 6. **Comparison of effects of different treatments on cell surface translocation of two THP mutants.** *A* and *B*, results summarized from FACS of MDCK cells harboring the two THP mutants that had been treated with various conditions. *C* and *D*, extent of THP released into the cultured media subsequent to various treatments. *NT*, no treatment; *LT*, low temperature; *GLY*, glycerol; *Tha*, thapsigargin; *PR*, probenecid. Data were means ± S.E.

mg/ml probenecid). Of the three chemicals tested, thapsigargin was highly cytotoxic; the rest were well tolerated by the cultured cells. 4-PBA had comparable effects on reducing perinuclear staining and increasing the surface labeling of both C126R and C217G (Fig. 5). Large sized and very strongly surface-labeled cells were observed with 4-PBA, a finding consistent with those previously published (34). To our surprise, probenecid, a drug that has been used empirically to lessen hyperuricemia (48), dramatically increased cell surface labeling of the THP mutants (Fig. 5). 4-PBA and probenecid also outperformed thapsigargin in elevating the levels of mutated THPs in the culture media to about 50% of the level of WT THP (Fig. 6, *B* and *D*).

Restoration of HSP70 Level Is Associated with Increased ER Exit and Surface Translocation of THP Mutants—To investigate whether the accumulation of THP mutants in the ER affected the levels of key molecular chaperones and, more importantly, whether chemical treatments that reduced mutant accumulation in the ER correlated with chaperone changes, we performed Western blotting and immunofluorescence staining of MDCK cells expressing the THP mutants. The steady-state levels of ER chaperones including ERp57 and calnexin were slightly lower in cells expressing the mutants (C126R and C217G) than in those expressing no THP, tagless THP, or differently tagged WT THP (Fig. 7*A*). The level of calreticulin did not seem to differ significantly. In striking contrast, there was a marked reduction of cytosolic chaperone HSP70 in cells expressing the two THP mutants (Fig. 7*A*). Cells harboring the two THP mutants and cultured under low temperature or in the presence of 4-PBA or probenecid had a complete restoration of the level of HSP70 (Fig. 7*B*). The results were confirmed by immunofluorescence staining, which showed strong cytoplasmic HSP70 localization with a filamentous configuration (Fig. 7*C*). These data suggest that the cytosolic HSP70 may play an important role in the refolding and ER exit of the THP mutants and in the improvement of their cell surface translocation. To further study whether the apparent disappearance of HSP70 from THP mutant-expressing cells was due to a bystander effect of increased proteasome degradation of trapped THP mutants, we treated mutant-expressing cells with a proteasome inhibitor, MG132 (43). This led to a marked accumulation of HSP70 (Fig. 7*D*). Unlike HSP70 in low temperature- and chemical chaperone-treated cells where it was largely cytoplasmic and filamentous, HSP70 in cells treated with MG132 was primarily perinuclear, appeared as aggregates, and had significant overlap with aggregated THP mutants (Fig. 7*D*). Additionally, the increased HSP70 in MG132-treated cells was not associated with an increased cell surface staining of mutant THP as mutant THP remained primarily perinuclear as aggregates.

DISCUSSION

Location of THP Mutation and Severity of Phenotype—In an effort to better understand the cellular mechanisms whereby THP mutations exert their pathogenic effects, we concentrated on two cysteine-altering mutations that were found in THP-associated kidney diseases (28, 44). We selected these two mutations because of their discrete locations with one in the domain of 8 cysteines (C126R) and the other outside of it (C217G) (23). However, we were still surprised by the extent to which these two mutants differed in their ER retention, apoptosis induction, apical surface targeting, natural and PLC-assisted release into the culture media, and entrapment of co-expressed wild-type THP. In all these respects, C217G triggered far more

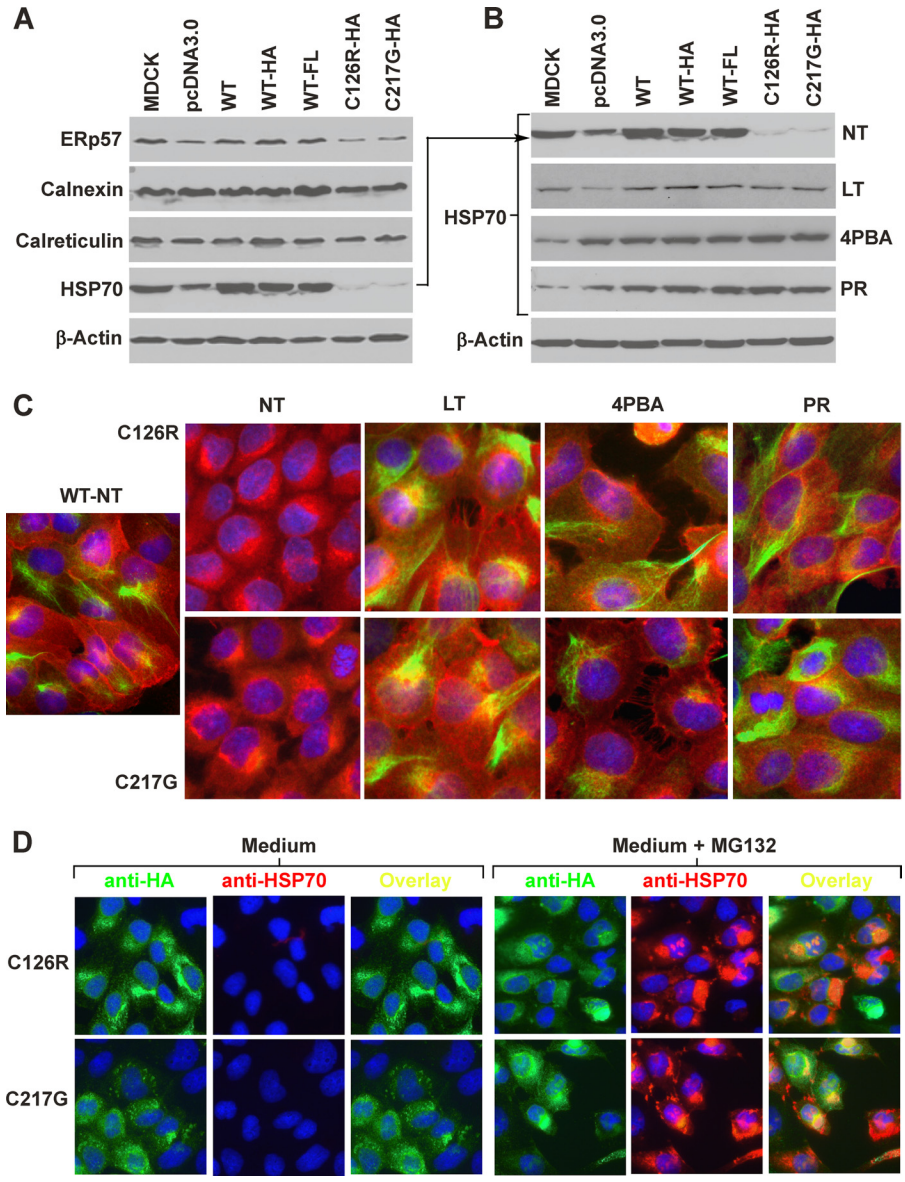

FIGURE 7. **Effects of different treatments on expression of ER molecular chaperones.** *A*, determination of the steady-state levels of ERp57, calnexin, calreticulin, and HSP70 in untransfected MDCK cells or MDCK cells stably transfected with vector only (*pcDNA3.0*), WT THP, HA-tagged WT THP, FL-tagged WT THP, HA-tagged THP mutant (C126R), or another HA-tagged THP mutant (C217G). *B*, treatment with low temperature (*LT*), 4-PBA, and probenecid (*PR*) dramatically up-regulated the level of HSP70 in cells expressing the THP mutants. *C*, immunofluorescence staining of HSP70 in untreated and chemical chaperone-treated cells. MDCK cells stably transfected with WT THP and THP mutants (C126R or C217G) underwent no treatment (*NT*) or low temperature, 4-PBA, or probenecid treatment. The cells were permeabilized and doubly stained with anti-THP (*red*) and anti-HSP70 (*green*). *D*, MDCK cells stably transfected with C126R-HA or C217G-HA were cultured in the presence of DMEM only or DMEM plus proteasome inhibitor MG132. The cells were then fixed, permeabilized, and double immunofluorescence-stained with anti-HA (*green*) and anti-HSP70 (*red*).

severe phenotypes than did C126R (Figs. 1–3). Thus, our data provide experimental evidence supporting the idea from sequence analysis that the highly conserved cysteines within D8C may be more functionally pivotal and that their mutations may cause worse structural deformation of THP and functional abnormalities in the mutant-bearing cells.

Although not directly addressing the importance of D8C, previous reports did note similar location-dependent effects involving cysteine and non-cysteine mutations of THP. For instance, Jennings *et al.* (36) found THP mutants C77Y and N128S to be targeted mostly to the apical membrane of the transiently transfected renal epithelial cell line LLC-PK1. In contrast, Williams *et al.* (33) showed that all but one of the THP mutants they expressed in HeLa cells (*i.e.* C32W, R185G, D196N, C217W, and C223R) were trapped in the ER and failed to reach the plasma membrane. Quantitative experiments were not carried out, however, to determine whether the two cysteine-altering mutations, *i.e.* C217W and C223R located in D8C, fared worse in surface translocation than C32W located outside D8C. Interestingly, the only mutant, G488R, that translocated very efficiently to the cell surface was located in the zona pellucida domain (33). In another study, Bernascone *et al.* (6) transiently transfected HEK293 and MDCK cells with 12 THP mutants. They noted considerable variability of the mutants to translocate to the plasma membrane with M229R being 3 times as efficient as N128S. Because M229 is inside

D8C, this raises the possibility that the more deleterious effects caused by cysteine-altering mutations within D8C might not apply to non-cysteine residues. Finally, Vylet'al *et al.* (30) categorized THP mutants into two groups based on results from transfecting HEK293, MDCK, CHO, and AtT-20 cells: (i) those capable of translocating to the cell surface (C32Y, M229R, and C317Y) and (ii) those that were primarily retained in the ER (C126R, P236L, and S273F). Because the C217G mutation was not analyzed and quantitative assays were not performed, it was unclear from this study whether D8C cysteines were more important structurally than the cysteines located elsewhere. Nevertheless, the data from the independent investigators, together with ours, are strongly suggestive of a location-dependent effect of THP mutations on the severity of the cellular phenotype. Although the exact mechanism(s) underlying this phenomenon requires further study, it is conceivable that mutations at different locations may affect the conformation of THP to different extents. This could translate into different degrees of ER retention and ability to transit to the apical surface. Mutations that are less capable of exiting the ER are likely to elicit more severe ER stress and apoptosis, a scenario entirely supported by our finding (Fig. 3). It should be noted that, given these interesting results from the cell culture studies, *in vivo* work such as transgenic expression of different mutants to independently demonstrate the location dependence has yet to be carried out. Additionally, the clinical relevance of this location-phenotype relationship also needs to be validated. THP mutations are known to be associated with at least three clinically distinct diseases: familial juvenile hyperuricemic nephropathy, medullary cystic kidney disease type II, and glomerulocystic disease (27, 28, 31). Within each disease entity, the onset, severity, renal pathology, and timeline of progression to renal failure also vary considerably among different patient families. The reason why different mutations in a single (THP) gene can cause such a remarkable degree of phenotypic variability is currently unknown. Clearly, more systematic studies are required to determine whether at least some of these variations are due to site-dependent mutational events.

Intermolecular Interaction in ER as Factor of Dominant Negativity of THP Mutation—It is well known that THP mutation-related diseases are inherited in an autosomal dominant manner. It also has been shown in patients bearing THP mutations that not only is the mutated THP absent in the urine but the WT THP is markedly reduced (35, 37, 38). Every autosome-encoded gene has two alleles, both of which are transcribed in most situations (49). Because of these reasons, the profound reduction of the WT THP in patients' urine implies that either the synthesis of WT THP is adversely affected or the mutant THP can interact with the WT THP at some point in their biosynthesis and intracellular trafficking. Prior to our study, however, this important issue had not been addressed. Our co-transfection experiments demonstrated that the mutant THP can in fact bind to WT THP and cause the latter to be trapped in the ER. This was evidenced by (i) double immunofluorescence staining of co-transfected MDCK cells showing perinuclear accumulation of the WT THP, (ii) co-IP and reverse co-IP experiments showing direct binding between mutant and WT THP and incomplete *N*-glycosylation of WT THP, and (iii) reduced release of WT THP by PLC treatment in co-transfected cells. The retention of WT THP by mutant THP via specific intermolecular interactions was also supported by the fact that the cell surface translocation of endogenously expressed GP135, a cell surface membrane marker of MDCK cells (41), was largely unaffected by the THP mutants (Fig. 2*B*). It should be noted, however, that the retention effect of mutant THP toward WT THP was incomplete, resulting in a portion of WT THP to be localized to the cell surface. Such "escaped" THP, although quantitatively insufficient, may still perform certain levels of physiological functions. The varied amounts of WT THP that are capable of escaping mutant THP could be another basis for varied disease entities and phenotypic severity of THP mutation-related diseases. Based on this reasoning, mutations affecting both THP gene alleles would not have the "escaping" effect and consequently may have a more severe phenotype. This prediction turned out to be exactly the case. Rezende-Lima *et al.* (50) showed in a family with familial juvenile hyperuricemic nephropathy and medullary cystic kidney disease type II that homozygous carriers of C255Y had a much earlier onset of hyperuricemia and faster progression to end stage renal disease than the heterozygous carriers of the same mutation. By demonstrating a trapping effect of a mutated THP toward its wild-type counterpart, we are by no means excluding the global effects of the cytotoxicity of the mutant on the protein synthesis and trafficking in the host cells. It is likely that the reduced cell surface translocation of the wild-type THP is a combined result of both the cytotoxicity and the trapping effect of the THP mutants.

Rescue of THP Mutants by Chemical Chaperones—It is becoming increasingly clear that THP mutations, like mutations of several other surface membrane proteins/receptors that cause ER storage diseases, are not by themselves "loss-of-function" mutations, but they rather impact indirectly on the cellular functions by triggering ER stress/apoptosis and impeding protein translocation to the cell surface (4, 28, 51, 52). For this reason, conditions that help improve the folding of mutated THP would be expected to have dual beneficial effects on relieving the ER stress and increasing the rate of apical translocation of mutant and WT THP. Toward this goal, we evaluated a range of conditions on stably transfected MDCK cells expressing the C126R or C127G THP mutant. Among the conditions tested were (i) low permissive temperature (30 °C), which facilitates the escape of mutant proteins from the quality control system of the rough ER (39, 53); (ii) cellular osmolytes (glycerol, TMAO, and DMSO), a group of chemical chaperones that are capable of hydrating the polypeptide side chains and stabilizing mutant proteins to their native confirmation (39, 40); (iii) thapsigargin, a small molecule inhibitor of Ca^{2+}-ATPase that reduces available Ca^{2+} in the ER and hence inhibits the Ca^{2+}-dependent quality control mechanism by the molecular chaperones (45); (iv) 4-PBA, a chemical chaperone that stimulates heat shock protein expression (46); and (v) probenecid, a uricosuric drug that has been used clinically to treat hyperuricemia (47) but has never been shown to act as a chaperone. Of note, all conditions were well tolerated by cultured MDCK cells except thapsigargin, which was highly cytotoxic, causing severe cell death and detachment. Although an effec-

tive agent for other protein mutants (45, 54), such a high level of cytotoxicity might preclude thapsigargin from clinical use for THP-associated renal diseases. Although all treatments increased the number of cells expressing the two mutant THPs on the cell surface (ranging from 30 to 65% of that of WT THP), the concentrations of THP in the culture media, which we believe is a more accurate indicator for the amount of cell surface THP, are more condition-dependent. Compared with the WT THP, low temperature, TMAO, and DMSO only marginally increased the THP secretion. Glycerol was more effective for C126R than for C217G, raising the medium concentration to about 45% of the WT THP. These data indicate that cellular osmolytes, which improved the cell surface expression of mutated αA-crystallin, cystic fibrosis transmembrane conductance regulator, AQP2, and podocin (40, 55–57), are not as effective for THP mutations. In contrast, 4-PBA raised the medium concentrations of C126R and C217G to 70 and 40% of WT THP, respectively, a remarkable improvement over the concentrations of these two mutants under non-treated conditions (6 and 2%, respectively). Our results from 4-PBA treatment are in general agreement with an earlier report showing a ~30% improvement of THP secretion of a deletion mutant (529_555 del) and a missense mutant (G443A) of THP (34).

We were most intrigued by the surprising effects of probenecid on the two THP mutants. At a 1 mg/ml (3.5 μM) concentration, probenecid had an effect comparable with 4-PBA on C126R and was slightly more effective than 4-PBA on C217G. Although probenecid is used clinically to reduce the serum level of uric acid in disease entities now known to be caused by THP mutations (27), protein folding was not among the postulated mechanisms. Instead, the therapeutic effect of probenecid was attributed to its ability to bind and inhibit organic anion transporters responsible for uric acid reabsorption in the proximal tubules (58). By demonstrating that probenecid can also enhance the folding and apical translocation of mutated THP here, our results reveal a novel mechanism by which probenecid reduces serum uric acid in patients with THP-associated diseases by acting directly on and relieving the stress of the cells of the thick ascending limb of the loop of Henle that harbor the THP mutations. It will be interesting to see whether the effects we observed here with cultured cells could be reproduced with *in vivo* models and humans.

Potential Role of Cytosolic HSP70 in Refolding THP Mutants—Although molecular chaperones play crucially important roles in protein folding and quality control mechanisms (59–61), their involvement, or the lack thereof, in misfolded THP response and rescue has not been explored. By assessing the chaperone expression using Western blotting analysis of MDCK cells stably expressing the C126R and C217G THP mutants, we found that the level of HSP70 was markedly depressed in mutant-expressing cells compared with the WT controls (Fig. 7, *A* and *B*). This profound reduction of cytosolic HSP70 might be related to a bystander effect of heightened proteasomal degradation triggered by the mutated THP that was exported out of the rough ER. Indeed, blocking proteosomal protein degradation using a specific inhibitor, MG132, led to a marked perinuclear accumulation of HSP70 along with aggregated THP mutants in mutant-expressing cells (Fig. 7*D*). The MG132-caused increase of cytosolic HSP70, however, was not associated with an improved cell surface translocation of the THP mutants, suggesting that raising the level of HSP70 by blocking proteosomal degradation alone without improving mutant folding does not significantly improve mutant targeting to the cell surface. By contrast, treatment of the mutant-expressing cells with low temperature, 4-PBA, and probenecid not only increased the cytosolic level of HSP70 but restored its cytosolic localization to resemble that of WT THP-expressing cells (Fig. 7*C*). As noted, these changes were associated with significantly improved cell surface translocation of the THP mutants (Figs. 4–6 and 7*C*). Therefore, the pharmacological treatments might have improved the folding of the THP mutants and accelerated their outward movement along the secretory pathway, events that can in turn relieve the sequestration and proteasomal degradation of cytosolic HSP70. These chemical chaperones are particularly attractive from a therapeutic standpoint as they might add to the heretofore relatively limited treatment repertoire for THP mutation-associated renal diseases.

Although not as profound as the changes in HSP70, there was also a reduction of ER chaperones including ERp57 and calnexin in cells expressing the THP mutant. The reason for this is presently unclear, but it could be related to the fact that these two proteins form a complex that is involved in disulfide formation of Asn-linked glycoproteins. Because THP is a cysteine-rich, heavily Asn-glycosylated protein, ERp57 and calnexin are likely involved in its folding under normal circumstances. When a mispaired cysteine exits, as occurs in THP mutants, the association between the mutant THP and the ERp57-calnexin complex may be prolonged, thus triggering ER-associated degradation, leading to a reduction of these chaperones. This is akin to a situation found with a mutated von Willebrand factor (62). Additional experiments are clearly warranted to tease out the exact mechanisms leading to the changes we observed in cytosolic and ER chaperones and the relative contribution of their restored levels to improved folding of mutated THP.

REFERENCES

1. Serafini-Cessi, F., Malagolini, N., and Cavallone, D. (2003) Tamm-Horsfall glycoprotein: biology and clinical relevance. *Am. J. Kidney Dis.* **42,** 658–676
2. Kumar, S., and Muchmore, A. (1990) Tamm-Horsfall protein—uromodulin (1950–1990). *Kidney Int.* **37,** 1395–1401
3. Devuyst, O., Dahan, K., and Pirson, Y. (2005) Tamm-Horsfall protein or uromodulin: new ideas about an old molecule. *Nephrol. Dial. Transplant.* **20,** 1290–1294
4. Rampoldi, L., Scolari, F., Amoroso, A., Ghiggeri, G., and Devuyst, O. (2011) The rediscovery of uromodulin (Tamm-Horsfall protein): from tubulointerstitial nephropathy to chronic kidney disease. *Kidney Int.* **80,** 338–347
5. Malagolini, N., Cavallone, D., and Serafini-Cessi, F. (1997) Intracellular transport, cell-surface exposure and release of recombinant Tamm-Horsfall glycoprotein. *Kidney Int.* **52,** 1340–1350
6. Bernascone, I., Vavassori, S., Di Pentima, A., Santambrogio, S., Lamorte, G., Amoroso, A., Scolari, F., Ghiggeri, G. M., Casari, G., Polishchuk, R., and Rampoldi, L. (2006) Defective intracellular trafficking of uromodulin mutant isoforms. *Traffic* **7,** 1567–1579
7. Zaucke, F., Boehnlein, J. M., Steffens, S., Polishchuk, R. S., Rampoldi, L., Fischer, A., Pasch, A., Boehm, C. W., Baasner, A., Attanasio, M., Hoppe, B., Hopfer, H., Beck, B. B., Sayer, J. A., Hildebrandt, F., and Wolf, M. T. (2010)

Uromodulin is expressed in renal primary cilia and UMOD mutations result in decreased ciliary uromodulin expression. *Hum. Mol. Genet.* **19,** 1985–1997
8. Cavallone, D., Malagolini, N., and Serafini-Cessi, F. (2001) Mechanism of release of urinary Tamm-Horsfall glycoprotein from the kidney GPI-anchored counterpart. *Biochem. Biophys. Res. Commun.* **280,** 110–114
9. Fukuoka, S., and Kobayashi, K. (2001) Analysis of the C-terminal structure of urinary Tamm-Horsfall protein reveals that the release of the glycosyl phosphatidylinositol-anchored counterpart from the kidney occurs by phenylalanine-specific proteolysis. *Biochem. Biophys. Res. Commun.* **289,** 1044–1048
10. Rindler, M. J., Naik, S. S., Li, N., Hoops, T. C., and Peraldi, M. N. (1990) Uromodulin (Tamm-Horsfall glycoprotein/uromucoid) is a phosphatidylinositol-linked membrane protein. *J. Biol. Chem.* **265,** 20784–20789
11. Pak, J., Pu, Y., Zhang, Z. T., Hasty, D. L., and Wu, X. R. (2001) Tamm-Horsfall protein binds to type 1 fimbriated Escherichia coli and prevents E. coli from binding to uroplakin Ia and Ib receptors. *J. Biol. Chem.* **276,** 9924–9930
12. Mo, L., Zhu, X. H., Huang, H. Y., Shapiro, E., Hasty, D. L., and Wu, X. R. (2004) Ablation of the Tamm-Horsfall protein gene increases susceptibility of mice to bladder colonization by type 1-fimbriated Escherichia coli. *Am. J. Physiol. Renal Physiol.* **286,** F795–F802
13. Mo, L., Huang, H. Y., Zhu, X. H., Shapiro, E., Hasty, D. L., and Wu, X. R. (2004) Tamm-Horsfall protein is a critical renal defense factor protecting against calcium oxalate crystal formation. *Kidney Int.* **66,** 1159–1166
14. Mo, L., Liaw, L., Evan, A. P., Sommer, A. J., Lieske, J. C., and Wu, X. R. (2007) Renal calcinosis and stone formation in mice lacking osteopontin, Tamm-Horsfall protein, or both. *Am. J. Physiol. Renal Physiol.* **293,** F1935–F1943
15. Liu, Y., Mo, L., Goldfarb, D. S., Evan, A. P., Liang, F., Khan, S. R., Lieske, J. C., and Wu, X. R. (2010) Progressive renal papillary calcification and ureteral stone formation in mice deficient for Tamm-Horsfall protein. *Am. J. Physiol. Renal Physiol.* **299,** F469–F478
16. Raffi, H. S., Bates, J. M., Jr., Laszik, Z., and Kumar, S. (2009) Tamm-Horsfall protein protects against urinary tract infection by proteus mirabilis. *J. Urol.* **181,** 2332–2338
17. Bates, J. M., Raffi, H. M., Prasadan, K., Mascarenhas, R., Laszik, Z., Maeda, N., Hultgren, S. J., and Kumar, S. (2004) Tamm-Horsfall protein knockout mice are more prone to urinary tract infection: rapid communication. *Kidney Int.* **65,** 791–797
18. Raffi, H. S., Bates, J. M., Jr., Laszik, Z., and Kumar, S. (2005) Tamm-Horsfall protein acts as a general host-defense factor against bacterial cystitis. *Am. J. Nephrol.* **25,** 570–578
19. Köttgen, A., Hwang, S. J., Larson, M. G., Van Eyk, J. E., Fu, Q., Benjamin, E. J., Dehghan, A., Glazer, N. L., Kao, W. H., Harris, T. B., Gudnason, V., Shlipak, M. G., Yang, Q., Coresh, J., Levy, D., and Fox, C. S. (2010) Uromodulin levels associate with a common UMOD variant and risk for incident CKD. *J. Am. Soc. Nephrol.* **21,** 337–344
20. Sedor, J. R. (2010) Uromodulin and translational medicine: will the SNPs bring zip to clinical practice? *J. Am. Soc. Nephrol.* **21,** 204–206
21. Köttgen, A., Glazer, N. L., Dehghan, A., Hwang, S. J., Katz, R., Li, M., Yang, Q., Gudnason, V., Launer, L. J., Harris, T. B., Smith, A. V., Arking, D. E., Astor, B. C., Boerwinkle, E., Ehret, G. B., Ruczinski, I., Scharpf, R. B., Chen, Y. D., de Boer, I. H., Haritunians, T., Lumley, T., Sarnak, M., Siscovick, D., Benjamin, E. J., Levy, D., Upadhyay, A., Aulchenko, Y. S., Hofman, A., Rivadeneira, F., Uitterlinden, A. G., van Duijn, C. M., Chasman, D. I., Paré, G., Ridker, P. M., Kao, W. H., Witteman, J. C., Coresh, J., Shlipak, M. G., and Fox, C. S. (2009) Multiple loci associated with indices of renal function and chronic kidney disease. *Nat. Genet.* **41,** 712–717
22. Gudbjartsson, D. F., Holm, H., Indridason, O. S., Thorleifsson, G., Edvardsson, V., Sulem, P., de Vegt, F., d'Ancona, F. C., den Heijer, M., Wetzels, J. F.,Franzson, L., Rafnar, T., Kristjansson, K., Bjornsdottir, U. S., Eyjolfsson, G. I., Kiemeney, L. A., Kong, A., Palsson, R., Thorsteinsdottir, U., and Stefansson, K. (2010) Association of variants at UMOD with chronic kidney disease and kidney stones-role of age and comorbid diseases. *PLoS Genet.* **6,** e1001039
23. Yang, H., Wu, C., Zhao, S., and Guo, J. (2004) Identification and characterization of D8C, a novel domain present in liver-specific LZP, uromodulin and glycoprotein 2, mutated in familial juvenile hyperuricaemic nephropathy. *FEBS Lett.* **578,** 236–238
24. Jovine, L., Qi, H., Williams, Z., Litscher, E., and Wassarman, P. M. (2002) The ZP domain is a conserved module for polymerization of extracellular proteins. *Nat. Cell Biol.* **4,** 457–461
25. Schaeffer, C., Santambrogio, S., Perucca, S., Casari, G., and Rampoldi, L. (2009) Analysis of uromodulin polymerization provides new insights into the mechanisms regulating ZP domain-mediated protein assembly. *Mol. Biol. Cell* **20,** 589–599
26. Hart, T. C., Gorry, M. C., Hart, P. S., Woodard, A. S., Shihabi, Z., Sandhu, J., Shirts, B., Xu, L., Zhu, H., Barmada, M. M., and Bleyer, A. J. (2002) Mutations of the UMOD gene are responsible for medullary cystic kidney disease 2 and familial juvenile hyperuricaemic nephropathy. *J. Med. Genet.* **39,** 882–892
27. Bleyer, A. J., Hart, P. S., and Kmoch, S. (2010) Hereditary interstitial kidney disease. *Semin. Nephrol.* **30,** 366–373
28. Scolari, F., Caridi, G., Rampoldi, L., Tardanico, R., Izzi, C., Pirulli, D., Amoroso, A., Casari, G., and Ghiggeri, G. M. (2004) Uromodulin storage diseases: clinical aspects and mechanisms. *Am. J. Kidney Dis.* **44,** 987–999
29. Lens, X. M., Banet, J. F., Outeda, P., and Barrio-Lucía, V. (2005) A novel pattern of mutation in uromodulin disorders: autosomal dominant medullary cystic kidney disease type 2, familial juvenile hyperuricemic nephropathy, and autosomal dominant glomerulocystic kidney disease. *Am. J. Kidney Dis.* **46,** 52–57
30. Vylet'al, P., Kublová, M., Kalbácová, M., Hodanová, K., Baresová, V., Stibrková, B., Sikora, J., Hlková, H., Zivný, J., Majewski, J., Simmonds, A., Fryns, J. P., Venkat-Raman, G., Elleder, M., and Kmoch, S. (2006) Alterations of uromodulin biology: a common denominator of the genetically heterogeneous FJHN/MCKD syndrome. *Kidney Int.* **70,** 1155–1169
31. Cameron, J. S., and Simmonds, H. A. (2005) Hereditary hyperuricemia and renal disease. *Semin. Nephrol.* **25,** 9–18
32. Puig, J. G., Prior, C., Martínez-Ara, J., and Torres, R. J. (2006) Familial nephropathy associated with hyperuricemia in Spain: our experience with 3 families harbouring a UMOD mutation. *Nucleosides Nucleotides Nucleic Acids* **25,** 1295–1300
33. Williams, S. E., Reed, A. A., Galvanovskis, J., Antignac, C., Goodship, T., Karet, F. E., Kotanko, P., Lhotta, K., Morinière, V., Williams, P., Wong, W., Rorsman, P., and Thakker, R. V. (2009) Uromodulin mutations causing familial juvenile hyperuricaemic nephropathy lead to protein maturation defects and retention in the endoplasmic reticulum. *Hum. Mol. Genet.* **18,** 2963–2974
34. Choi, S. W., Ryu, O. H., Choi, S. J., Song, I. S., Bleyer, A. J., and Hart, T. C. (2005) Mutant Tamm-Horsfall glycoprotein accumulation in endoplasmic reticulum induces apoptosis reversed by colchicine and sodium 4-phenylbutyrate. *J. Am. Soc. Nephrol.* **16,** 3006–3014
35. Rampoldi, L., Caridi, G., Santon, D., Boaretto, F., Bernascone, I., Lamorte, G., Tardanico, R., Dagnino, M., Colussi, G., Scolari, F., Ghiggeri, G. M., Amoroso, A., and Casari, G. (2003) Allelism of MCKD, FJHN and GCKD caused by impairment of uromodulin export dynamics. *Hum. Mol. Genet.* **12,** 3369–3384
36. Jennings, P., Aydin, S., Kotanko, P., Lechner, J., Lhotta, K., Williams, S., Thakker, R. V., and Pfaller, W. (2007) Membrane targeting and secretion of mutant uromodulin in familial juvenile hyperuricemic nephropathy. *J. Am. Soc. Nephrol.* **18,** 264–273
37. Bleyer, A. J., Hart, T. C., Shihabi, Z., Robins, V., and Hoyer, J. R. (2004) Mutations in the uromodulin gene decrease urinary excretion of Tamm-Horsfall protein. *Kidney Int.* **66,** 974–977
38. Dahan, K., Devuyst, O., Smaers, M., Vertommen, D., Loute, G., Poux, J. M., Viron, B., Jacquot, C., Gagnadoux, M. F., Chauveau, D., Büchler, M., Cochat, P., Cosyns, J. P., Mougenot, B., Rider, M. H., Antignac, C., Verellen-Dumoulin, C., and Pirson, Y. (2003) A cluster of mutations in the UMOD gene causes familial juvenile hyperuricemic nephropathy with abnormal expression of uromodulin. *J. Am. Soc. Nephrol.* **14,** 2883–2893
39. Morello, J. P., Petäjä-Repo, U. E., Bichet, D. G., and Bouvier, M. (2000) Pharmacological chaperones: a new twist on receptor folding. *Trends Pharmacol. Sci.* **21,** 466–469
40. Ohashi, T., Uchida, K., Uchida, S., Sasaki, S., and Nihei, H. (2003) Intracellular mislocalization of mutant podocin and correction by chemical

chaperones. *Histochem. Cell Biol.* **119,** 257–264
41. Ojakian, G. K., and Schwimmer, R. (1988) The polarized distribution of an apical cell surface glycoprotein is maintained by interactions with the cytoskeleton of Madin-Darby canine kidney cells. *J. Cell Biol.* **107,** 2377–2387
42. Cavallone, D., Malagolini, N., Monti, A., Wu, X. R., and Serafini-Cessi, F. (2004) Variation of high mannose chains of Tamm-Horsfall glycoprotein confers differential binding to type 1-fimbriated Escherichia coli. *J. Biol. Chem.* **279,** 216–222
43. Lee, D. H., and Goldberg, A. L. (1998) Proteasome inhibitors: valuable new tools for cell biologists. *Trends Cell Biol.* **8,** 397–403
44. Turner, J. J., Stacey, J. M., Harding, B., Kotanko, P., Lhotta, K., Puig, J. G., Roberts, I., Torres, R. J., and Thakker, R. V. (2003) UROMODULIN mutations cause familial juvenile hyperuricemic nephropathy. *J. Clin. Endocrinol. Metab.* **88,** 1398–1401
45. Delisle, B. P., Anderson, C. L., Balijepalli, R. C., Anson, B. D., Kamp, T. J., and January, C. T. (2003) Thapsigargin selectively rescues the trafficking defective LQT2 channels G601S and F805C. *J. Biol. Chem.* **278,** 35749–35754
46. Choo-Kang, L. R., and Zeitlin, P. L. (2001) Induction of HSP70 promotes DeltaF508 CFTR trafficking. *Am. J. Physiol. Lung Cell. Mol. Physiol.* **281,** L58–L68
47. Chung, Y., Stocker, S. L., Graham, G. G., and Day, R. O. (2008) Optimizing therapy with allopurinol: factors limiting hypouricemic efficacy. *Am. J. Med. Sci.* **335,** 219–226
48. Bleyer, A. J., and Hart, T. C. (2006) Genetic factors associated with gout and hyperuricemia. *Adv. Chronic Kidney Dis.* **13,** 124–130
49. Buckland, P. R. (2004) Allele-specific gene expression differences in humans. *Hum. Mol. Genet.* **13,** Spec. No. 2, R255–R260
50. Rezende-Lima, W., Parreira, K. S., García-González, M., Riveira, E., Banet, J. F., and Lens, X. M. (2004) Homozygosity for uromodulin disorders: FJHN and MCKD-type 2. *Kidney Int.* **66,** 558–563
51. Nasr, S. H., Lucia, J. P., Galgano, S. J., Markowitz, G. S., and D'Agati, V. D. (2008) Uromodulin storage disease. *Kidney Int.* **73,** 971–976
52. Ron, D., and Walter, P. (2007) Signal integration in the endoplasmic reticulum unfolded protein response. *Nat. Rev. Mol. Cell Biol.* **8,** 519–529
53. Arakawa, T., Ejima, D., Kita, Y., and Tsumoto, K. (2006) Small molecule pharmacological chaperones: From thermodynamic stabilization to pharmaceutical drugs. *Biochim. Biophys. Acta* **1764,** 1677–1687
54. Robben, J. H., Sze, M., Knoers, N. V., and Deen, P. M. (2006) Rescue of vasopressin V2 receptor mutants by chemical chaperones: specificity and mechanism. *Mol. Biol. Cell* **17,** 379–386
55. Gong, B., Zhang, L. Y., Pang, C. P., Lam, D. S., and Yam, G. H. (2009) Trimethylamine N-oxide alleviates the severe aggregation and ER stress caused by G98R alphaA-crystallin. *Mol. Vis.* **15,** 2829–2840
56. Fischer, H., Fukuda, N., Barbry, P., Illek, B., Sartori, C., and Matthay, M. A. (2001) Partial restoration of defective chloride conductance in DeltaF508 CF mice by trimethylamine oxide. *Am. J. Physiol. Lung Cell. Mol. Physiol.* **281,** L52–L57
57. Tamarappoo, B. K., and Verkman, A. S. (1998) Defective aquaporin-2 trafficking in nephrogenic diabetes insipidus and correction by chemical chaperones. *J. Clin. Investig.* **101,** 2257–2267
58. Hosoyamada, M., Ichida, K., Enomoto, A., Hosoya, T., and Endou, H. (2004) Function and localization of urate transporter 1 in mouse kidney. *J. Am. Soc. Nephrol.* **15,** 261–268
59. Morano, K. A. (2007) New tricks for an old dog: the evolving world of Hsp70. *Ann. N.Y. Acad. Sci.* **1113,** 1–14
60. Brodsky, J. L. (2007) The protective and destructive roles played by molecular chaperones during ERAD (endoplasmic-reticulum-associated degradation). *Biochem. J.* **404,** 353–363
61. Määttänen, P., Gehring, K., Bergeron, J. J., and Thomas, D. Y. (2010) Protein quality control in the ER: the recognition of misfolded proteins. *Semin. Cell Dev. Biol.* **21,** 500–511
62. Allen, S., Goodeve, A. C., Peake, I. R., and Daly, M. E. (2001) Endoplasmic reticulum retention and prolonged association of a von Willebrand's disease-causing von Willebrand factor variant with ERp57 and calnexin. *Biochem. Biophys. Res. Commun.* **280,** 448–453